Fluids adsorbed in narrow pores: phase equilibria and structure

1990 J. Phys.: Condens. Matter 2 8989

(http://iopscience.iop.org/0953-8984/2/46/001)

J. Phys.: Condens. Matter. 2 (1990) 8989–9007. Printed in the UK

REVIEW ARTICLE

Fluids adsorbed in narrow pores: phase equilibria and structure

R Evans
H H Wills Physics Laboratory, University of Bristol, Bristol BS8 1TL, UK

Received 27 July 1990

Abstract. When gases or liquids are adsorbed in narrow pores or capillaries their properties are significantly different from those in a bulk phase. This article reviews recent developments in the statistical theory and computer simulation of simple fluids confined in model pores, emphasizing the microscopic structure and phase equilibria. The structure reflects the packing of atoms or molecules in confining geometries while the phase behaviour reflects the presence of surface and bulk contributions to the fluid's free energy. Confinement shifts first-order transitions, such as condensation or freezing, away from their location in bulk; it also alters the location and nature of the bulk critical point reducing the effective dimensionality. Sometimes surface phase transitions such as layering and prewetting compete with shifted bulk transitions giving rise to rich phase diagrams. The extent to which the theorists' results for fluids in single idealized pores might be relevant for solvation force studies probing liquids between crossed mica cylinders and for gas adsorption studies in real mesoporous solids such as VYCOR is mentioned briefly.

1. Introduction

The phenomenon of the rise, against gravity, of a liquid in a vertical capillary is one of the most striking manifestations of surface tension, providing direct evidence for the existence of attractive intermolecular forces [1]. The successful understanding of capillary rise, due to Young and Laplace, was a triumph of early 19th century physics. However, the macroscopic concepts of surface tension, contact angle and pressure difference across a curved meniscus, which form the basis of the classical theory of capillarity, are of limited applicability once the dimensions of the capillary cannot be regarded as macroscopic. Microscopic treatments are necessary when a significant fraction of the volume of the capillary is occupied by fluid whose local density $\rho(\boldsymbol{r})$ is, as a result of the confining effects of the walls, different from that in bulk. Such situations arise for fluids adsorbed in porous structures whose pore sizes are of the order of several molecular diameters, e.g. in zeolites, VYCOR glass, carbon powders and clays, where typical sizes may lie in the range 10–200 Å.

Despite the importance of fluids in porous media for several branches of surface chemistry and physics, fundamental understanding of gases and liquids confined in very narrow pores did not begin to emerge until quite recently. Progress had to await the advances made during the last decade or so in the statistical mechanical theory and computer simulation of fluid interfaces. Techniques introduced for liquid–gas interfaces [1] and for adsorption at solid substrates [2] have been extended to the problem of fluids

0953-8984/90/468989 + 19 $03.50

in idealized, *model* pores. The main thrust of recent research deals with the following types of questions: (i) To what extent can notions of bulk phase equilibria be employed in confined systems? For example, do the condensation and freezing transitions persist in narrow capillaries? Are there well-defined critical points for a confined fluid? Do new phase transitions resulting from the interplay between bulk and surface ordering occur and if so, what is their nature? (ii) What is the microscopic structure of a confined gas or liquid and how does this depend upon the geometry of the pore and the nature of the confining substrate? When does quasi-two- or one-dimensional ordering occur? This is equivalent to asking: what are the effects of packing constraints and substrate forces on the statistical arrangements of molecules in the fluid? (iii) How are transport properties such as diffusion and viscosity affected by confinement? Since the answers to these questions cannot be obtained easily from experiment, it is not surprising that the theoretician and the computer simulator have had free rein. Nevertheless, one should emphasize that one of the ultimate aims of such studies is to provide fundamental theoretical input for many practical problems such as the interpretation of gas adsorption measurements for porous substrates [3], processes involving fluid flow in porous media and interpreting solvation force measurements for liquids contained between crossed mica cylinders. This last technique is growing in importance as it provides quantitative information about liquid mediated forces between two substrates separated by microscopic distances [4].

The present article attempts to give the flavour of some of the recent work in this field. It is not intended to be comprehensive. Emphasis is placed on phase equilibria, microscopic structure and adsorption phenomena; the choice reflects the author's own interests. Transport properties, in particular, warrant a separate discussion [5, 6].

2. Model pores and model fluids

2.1. Confining geometries

Although spherical cavities have been considered as a crude model for certain zeolites [7], two main geometries are favoured: slits and cylinders.

In the former the fluid is confined between two parallel solid substrates which are of (infinite) area A, but which are separated by a finite distance L—see figure 1. For the open-cylinder geometry the interior radius R_c is finite but the length becomes infinite. One imagines a reservoir of fluid in contact with either pore so that fluid molecules can be adsorbed on the interior substrate of the cylinder and on the two interior substrates of the slit. The chemical potential μ and temperature T of the confined fluid are fixed by the reservoir. Increasing μ, or the pressure of the fluid in the reservoir, will usually lead to an increase in the number of fluid molecules adsorbed. Provided the substrates can be regarded as rigid (homogeneous and inert) on suitable time and energy scales, these can be viewed as walls that merely exert an external potential $V(\boldsymbol{r})$ on fluid molecules. The basic statistical mechanical problem then reduces to one of determining the equilibrium and, possibly, the non-equilibrium properties of a fluid in the presence of confining external potentials. The spatial inhomgeneity of the average *fluid* density $\rho(\boldsymbol{r})$ is governed by that of the confining potential.

2.2. Continuum models

Most attention has been focussed on *simple* fluids, e.g. rare gases or small, non-polar molecules. These are often modelled by a Lennard-Jones 12–6 fluid–fluid intermolecular

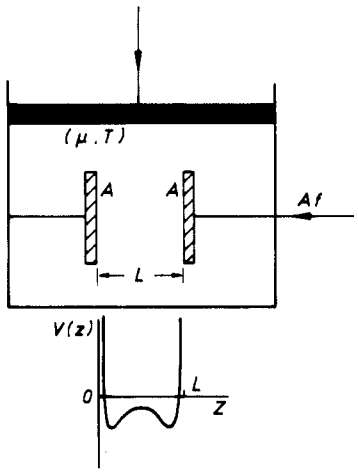

Figure 1. System of two adsorbing substrates of surface area A, repelling with force Af. $V(z)$ is the confining potential experienced by a molecule in the fluid.

pair potential $\Phi_{LJ}(r) = 4\varepsilon_{LJ}[(\sigma_{LJ}/r)^{12} - (\sigma_{LJ}/r)^6]$, with diameter σ_{LJ} and well-depth ε_{LJ} chosen to mimic a particular fluid. The substrate potential is chosen to be as simple as possible, whilst still retaining both attractive and repulsive components for the fluid molecules. In most calculations the variation of the potential parallel to the substrate, arising from the 'corrugations' associated with the crystalline arrangement of substrate molecules, is ignored so that $V(\boldsymbol{r}) \rightarrow V(z)$ and $\rho(\boldsymbol{r}) \rightarrow \rho(z)$ for slits whilst $V(\boldsymbol{r}) \rightarrow V(R)$ and $\rho(\boldsymbol{r}) \rightarrow \rho(R)$ for a cylinder; only variation normal to the now structureless wall is included. The neglect of corrugations can be significant, especially for the structure of the first adsorbed monolayer and for freezing of the layers [8, 9]. Moreover, in the limit where the pore size corresponds to a few (fluid) molecular diameters, specific adsorption sites and specific packing constraints will determine the details of the density variation and control the nature of the adsorption. Nevertheless, comparison of simulation results for supercritical liquids confined in corrugated and uncorrugated (structureless) slits [10] show that the latter often provide a realistic description of adsorption, even for L as small as 2.5 molecular diameters.

A well-studied model is the 9–3 potential $V^s(z) = 2\varepsilon_w[\frac{2}{15}(\sigma_w/z)^9 - (\sigma_w/z)^3]$ obtained by integrating the Lennard-Jones 12–6 wall-molecule–fluid-molecule pair potential over the transverse (x, y) directions of a single wall, assuming a constant wall density n_w. Increasing the strength parameter, ε_w, which is proportional to n_w, increases wall–fluid attraction, favouring increased adsorption. σ_w measures the range of wall–fluid repulsive forces. For the slit with identical walls [11] $V(z) = V^s(z) + V^s(L - z)$ (see figure 1), while for the cylinder the potential $V(R)$ is more complicated [12, 13]. Even simpler potentials are sometimes employed. For example, purely repulsive hard-sphere fluids and hard walls have been considered. While such idealized models are not intended to mimic any real confined fluid, rigorous results for certain properties can sometimes be obtained and these provide insight into fundamental issues [14].

2.3. Lattice models

Lattice gas models of confined fluids can be traced back to papers by Hill [15] and Nicholson [16]. In slit geometry the space between the parallel walls is filled by a lattice, simple-cubic say, with $L \equiv Na$ and $A \equiv M^2a^2$: a is the lattice spacing. The number of

layers normal to the walls, N, is finite while $M \to \infty$. Sites on the lattice may or may not be occupied by particles. In the simplest (Ising) version only nearest-neighbour interactions are included so that 'bonds' of energy $-\varepsilon$ ($\varepsilon > 0$) occur when neighbouring sites are occupied. The properties of the *bulk* (Ising) lattice gas, when no surfaces are present, are very well known. Below the critical temperature, $T_{c,\infty}$, where $k_B T_{c,\infty}/\varepsilon = 1.1279$ for simple cubic, a sparsely occupied 'gas' phase coexists with a densely occupied 'liquid' phase at chemical potential $\mu_{sat} = -3\varepsilon$, independent of T. The corresponding average occupancy, or density, ρ against T phase diagram is symmetric about $\rho = \rho_c = \frac{1}{2}$. Although such a coexistence curve is a crude representation of that of a real fluid, it does contain the essential physical features. In addition, the critical point behaviour of real fluids is known to lie in the three-dimensional Ising universality class [17], so the lattice model does incorporate the correct critical exponents for bulk fluids.

For the confined lattice gas the Hamiltonian is

$$H = -\varepsilon \sum_{\langle jk,j'k' \rangle} s_{jk} s_{j'k'} + \sum_{j=1}^{N} V_j \sum_k s_{jk} \tag{1}$$

where the occupancy variable $s_{jk} = 1$ if the kth site in the jth layer is occupied and is zero if this is empty. The first term in (1) is a sum over all nearest-neighbour pairs of sites while in the second term $V_j = V_j^s + V_{N+1-j}^s$ is the total potential experienced by a particle in layer j due to the walls. The single-wall potential $V_j^s = V^s(z_j)$ is assumed independent of x and y; it may take the integrated 9–3 or a closely related form. Sometimes free-edge boundary conditions are employed so that $V_j^s \equiv 0$ for all j, corresponding to a free finite film, with no modifications due to wall effects. Alternatively, extremely localized surface fields can be introduced which couple only to particles in the surface layers $j = 1$ and $j = N$: $V_j^s = V_1 \delta_{j1}$. Such a prescription is borrowed from the study of magnetic films where a localized surface magnetic field h_1 acting only on spins in the surface layers can be envisaged.

The advantage of lattice models of this type is that their equilibrium properties are amenable to extremely detailed investigation. In particular, extensive Monte Carlo simulations can be performed for system sizes that are not yet feasible for continuum fluids. The ability to study large systems is especially important when attempting to ascertain details of phase diagrams and the nature of any criticality that might occur. It is expected that phase transitions and adsorption phenomena found in lattice models should have rather direct counterparts in the continuum case. This expectation is confirmed for most surface phase transitions, especially wetting phenomena, at single substrates—see the reviews [18, 19] and there is growing evidence that it is correct for confined fluids. Of course, the Ising version of the lattice gas model does not incorporate a crystalline phase so it cannot be used to investigate possible capillary freezing transitions. Lattice models that do incorporate three bulk phases, i.e. a triple point, do exist, but these have not been applied systematically to confined systems. The other failing of the lattice models is that they cannot provide a realistic description of the effects of packing constraints on the density profiles of a real fluid confined in a very narrow pore; the form of the profile depends on whether or not the width of the slit or radius of the cylinder is commensurate with an integral number of (fluid) molecular diameters [20]. By fixing particles on lattice sites, imposed short-ranged correlations are very different from thsoe that would occur in the real fluid.

2.4. Simulation and approximate theories

The simulation techniques are fairly standard. Monte Carlo has been implemented [21], using periodic boundary conditions in the x and y directions, for lattices with 32^2 or 64^2

sites per layer and N up to 61 layers. The average occupancy of each layer and the total susceptibility is monitored along with the average energy. Thermodynamic integrations along reversible paths yield the grand potential Ω for any phases that are present. Grand canonical Monte Carlo (GCMC) has been used for Lennard-Jones fluids in cylinders [22], with periodic boundary conditions along the cylinder axis z, and in slits [8, 23].† While this technique allows one to calculate Ω, i.e. it provides a means of locating phase transitions, it does not allow the direct observation of two phases, separated by a meniscus, in the same pore. Such observations can be made using molecular dynamics simulations in the canonical ensemble and these results [24] have provided much insight into the nature of adsorption hysteresis in cylindrical pores. Total density profiles $\rho(R, z)$ can be computed [24, 25].

Theoretical work for lattice models is based upon a simple mean-field approximation [26] for the grand potential function $\bar{\Omega}(\{\rho_j\})$ which upon minimization yields estimates of the average occupancy profile $\{\rho_j\}$ and of Ω. Approximate density functional theories [14] have proved extremely powerful for describing the structure, i.e. the density profile $\rho(\boldsymbol{r})$, and for determining the phase equilibria of confined continuum fluids. One considers a functional

$$\Omega_V[\rho] = \mathcal{F}[\rho] + \int d\boldsymbol{r}\, \rho(\boldsymbol{r})V(\boldsymbol{r}) - \mu \int d\boldsymbol{r}\, \rho(\boldsymbol{r})$$

which upon minimization provides a variational estimate for the grand potential of the fluid confined by the external potential $V(\boldsymbol{r})$. $\mathcal{F}[\rho]$ is the intrinsic Helmholtz free-energy functional [14]; it contains an ideal gas term in addition to all fluid–fluid contributions to the free energy. Since the latter are not known exactly for any realistic fluid, approximations must be made. Attractive forces are usually treated in mean-field fashion while repulsive forces are modelled by hard spheres. The simplest approximation for the hard-sphere free-energy functional is $\mathcal{F}_{hs}[\rho] = \int d\boldsymbol{r} f_{hs}(\rho(\boldsymbol{r}))$, where $f_{hs}(\rho)$ is the free-energy density of a *uniform* hard-sphere fluid of density ρ, which is known accurately. This local density approximation constitutes a zeroth-order, or van der Waals, theory for inhomogeneous fluids, which has shed new light on a variety of interfacial problems [14, 18, 19]. It accounts for phase transitions, albeit at the mean-field level, but fails to describe the short-ranged correlations, arising from packing effects, that produce oscillations in the density profile for liquids near walls. In order to account for structure in $\rho(\boldsymbol{r})$ a non-local theory is required for $\mathcal{F}_{hs}(\rho)$. Various theories exist [14] but the version that has been employed extensively for confined fluids is that due to Tarazona [27]. When tested against simulation this non-local theory has been found to be accurate, both for fluid structure and for phase equilibria [10, 25]. Integral equation techniques for inhomogeneous fluids have also been applied to confined systems. These have often proved accurate for the structure but many have difficulties in accounting for phase transitions [14]. Important recent work in this area can be found in [61, 62].

3. Thermodynamics of adsorption for a confined fluid

3.1. Adsorption and solvation force

Before describing the results of calculations for the models introduced above, it is instructive to consider the thermodynamics of confined fluids. The natural choice of

† A great number of Monte Carlo and molecular dynamics calculations of the density profile, adsorption and solvation force have been carried out for simple fluids in slits. We do not review this work in any detail. References to early papers can be found in [14, 23, 25].

thermodynamic potential appropriate to an open system of the type shown in figure 1 is the grand potential $\Omega = U - TS - \mu N$, where U is the total internal energy, S the total entropy and N the total number of fluid molecules or particles in the lattice model. Whereas in a bulk fluid $\Omega = -pV$, where p is the bulk pressure and V is the volume occupied by the fluid, Ω for a confined fluid has an extra (surface) contribution proportional to the total surface area. For the slit, an increment in grand potential is given by

$$d\Omega = -p\,dV - S\,dT - N\,d\mu + 2\gamma\,dA - Af\,dL. \tag{2}$$

The standard (bulk) terms are supplemented by a surface work term: 2γ is the total wall–fluid interfacial tension, and a term that represents the work done when the wall separation L is increased by an amount dL. It is supposed that the force Af is applied externally at both walls as in figure 1. The presence of two extra thermodynamic fields A and L has significant repercussions for phase equilibria; these extra fields may augment the Gibbs phase rule appropriate to a one-component bulk fluid leading to a rich phase diagram [28]. By introducing suitable dividing surfaces at each wall and defining surface excess functions, the Gibbs adsorption equation for a confined fluid can be derived [28]:

$$2\,d\gamma + 2s\,dT + \Gamma\,d\mu + f\,dL = 0 \tag{3}$$

where $\Gamma = -2(\partial\gamma/\partial\mu)_{T,L} \equiv (N - N_b)/A$ is the adsorption, i.e. the excess number of molecules per unit area measured with respect to the bulk fluid at fixed (μ, T). s is the excess entropy per unit area. In the limit $L \to \infty$, $\Gamma(L) \to \Gamma_1 + \Gamma_2$: the sum of the adsorptions at single walls. Similarly $2\gamma(L) \to \gamma_1 + \gamma_2$: the sum of the individual wall–fluid tensions. f is also an excess quantity; it can be expressed as a pressure difference:

$$f = -(1/A)(\partial\Omega/\partial L)_{\mu,T,A} - p.$$

Recall that p refers to the bulk fluid in the reservoir. Only in the limit $L \to \infty$ does $f(L) \to 0$. It is conventional to divide $f(L)$ into two contributions: (i) $f_{pp}(L)$ arising from the direct intermolecular forces between the material of the two walls or plates, which should be independent of (μ, T), and (ii) a remainder, usually called the *solvation force*, that is associated with plate–fluid and fluid–fluid forces. This second term is the one relevant for fluid phase equilibria. Measurements of the solvation force have been made for a variety of liquids between two crossed mica cylinders using the technique pioneered by Israelachvili and co-workers [4]. Although the geometry is not that of parallel plates—it is equivalent to that of a sphere, with large radius of curvature, approaching a flat surface—the force that is measured has the same thermodynamic interpretation as that given above for $f(L)$. Since the experiments claim to measure the solvation force for separations as small as 10 Å, with a resolution of about 1 Å, this technique constitutes an extremely important surface probe. A recent book [29] describes the work of the Russian school in this field.

It is clear that any fundamental theory for the force requires, as input, $\gamma(L)$, i.e. some means of determining the excess free energy of the confined fluid from first principles. One feature of the solvation force measurements that has attracted much interest is the observation of oscillations for small plate separations [4, 29, 30], the peaks being separated by about one (fluid) molecular diameter. The same packing effects which give rise to highly structured density profiles $\rho(z)$ produce oscillatory $f(L)$. This is most clearly illustrated for the case of a liquid confined by two hard walls. For this

idealized situation, the solvation force is given by the exact statistical mechanical formula [31, 14]

$$f(L) = k_B T(\rho_L(0^+) - \rho_\infty(0^+))$$

where $\rho_L(0^+)$ is the liquid density at contact with each wall in the confined system. $\rho_\infty(0^+)$ is the corresponding quantity for infinite wall separation. When $L \sim$ few molecular diameters $\rho_L(0^+)$ reflects the packing of liquid molecules. If $L \geqslant$ an integral number of diameters $\rho_L(0^+)$ is much larger than the unconfined density $\rho_\infty(0^+)$ and f is large and positive. When L is out of registry with the packing $\rho_L(0^+) < \rho_\infty(0^+)$ and f is negative. Oscillatory $f(L)$ then results. Softening the wall–fluid repulsive potential does not change the essential physics of this argument [14].

3.2. *Characterization of phase transitions*

We are now in a position to state how possible phase equilibria should be characterized for a confined fluid. Suppose two (confined) phases α and β coexist for certain values of μ, T and L. This requires $\Omega_\alpha = \Omega_\beta$ or, alternatively, $\gamma_\alpha = \gamma_\beta$ since the bulk contribution to Ω is the same for each phase. Effecting a change in μ, T and L at fixed wall area A in such a way that α and β remain in equilibrium ($d\gamma_\alpha = d\gamma_\beta$) gives from (3)

$$2(s_\alpha - s_\beta)\,dT + (\Gamma_\alpha - \Gamma_\beta)\,d\mu + (f_\alpha - f_\beta)\,dL = 0. \tag{4}$$

The shape of the α–β coexistence surface is determined by three Clapeyron equations [28], e.g.

$$(\partial L/\partial \mu)_T = -\Delta\Gamma/\Delta f \tag{5}$$

gives the slope of the coexistence curve at fixed T in terms of the difference in adsorption $\Delta\Gamma \equiv \Gamma_\alpha - \Gamma_\beta$ between the two phases and the difference $\Delta f \equiv f_\alpha - f_\beta$ between the solvation forces. If α and β both have the same symmetry (both are fluids, say) $\Delta\Gamma$ is a natural order parameter; note the analogy with the bulk liquid–gas transition where $\Delta\rho \equiv \rho_l - \rho_g$ is the order parameter [17]. This implies that a critical point of a confined fluid should occur when $\Delta\Gamma$ vanishes at a certain (T, μ_c, L_c). The precise condition is

$$(\partial\mu/\partial\Gamma)^c_{A,T,L_c} = (\partial^2\mu/\partial\Gamma^2)^c_{A,T,L_c} = 0 \qquad (\partial^3\mu/\partial\Gamma^3)^c_{A,T,L_c} \geqslant 0. \tag{6}$$

Rather than varying L and μ at fixed T we might fix L and vary μ and T. Conditions, analogous to (6), determine the location $(\mu_{c,L}, T_{c,L})$ of the 'capillary critical point' [28]. In general, this point will be different from the bulk liquid–gas critical point $(\mu_{c,\infty}, T_{c,\infty})$. The analogy with bulk can be taken further by noticing that $\Gamma(\mu)$ and $-2\gamma(\mu)$ play the role of the bulk density $\rho_b(\mu)$ and pressure $p(\mu)$ respectively (recall that $\rho_b = (\partial p/\partial\mu)_T$). Thus in a classical, mean-field theory we expect $\Gamma(\mu)$ to develop a loop for $T < T_{c,L}$ as shown in figure 2(*a*). On increasing the temperature T the loop shrinks and the jump $\Delta\Gamma$ at the first-order transition decreases. Eventually at $T_{c,L}$ the jump vanishes and $(\partial\Gamma/\partial\mu)$ diverges as in figure 2(*b*). For $T > T_{c,L}$, Γ usually increases monotonically with μ (figure 2(*c*)). But Δf is just as good an order parameter as $\Delta\Gamma$ and the conditions for capillary criticality may also be expressed in terms of f. The classical picture of criticality that is described in figure 2 neglects the effects of critical fluctuations and we shall see that,

because of reduced dimensionality of the fluid, these effects are very important in confined fluids and the classical description becomes inaccurate near the critical point.

4. Capillary condensation: the shifted bulk transition

4.1. Macroscopic treatment

The best known example of a phase transition for a confined fluid is that of capillary condensation: the phenomenon whereby a gas at chemical potential $\mu < \mu_{sat}$ condenses to a dense, liquid-like phase that fills the pore. Capillary condensation has long been invoked [32] in the interpretation of the gas adsorption isotherms measured for mesoporous solids [3]. However, the precise nature of this phenomenon has remained somewhat obscure until recently. In the limit of large slit width L, or cylinder radius R_c, the undersaturation at which condensation occurs can be obtained using macroscopic arguments. Then phase β corresponds to a dilute gas while α corresponds to the condensing 'liquid' phase. Each confined phase has a density profile $\rho(z)$ that is almost constant throughout the slit so that the grand potentials of the fluid phases within the slit are the sum of bulk and surface contributions:

$$\Omega_\beta \approx -pAL + 2\gamma_{w\beta}A \tag{7a}$$

and

$$\Omega_\alpha \approx -p_\alpha^+ AL + 2\gamma_{w\alpha}A. \tag{7b}$$

p is the pressure of bulk β (in the reservoir) while p_α^+ is the pressure of the α phase at the same chemical potential μ. Such a (liquid) phase is metastable in bulk and is associated with a density ρ_α^+ obtained by considering a van der Waals loop for $\mu(\rho)$ [28]. $\gamma_{w\alpha}$ and $\gamma_{w\beta}$ are the single wall interfacial tensions evaluated at $\mu_{sat}(T)$. Coexistence of α and β occurs when $\Omega_\alpha = \Omega_\beta$, i.e. when

$$p - p_\alpha^+ = (2/L)(\gamma_{w\beta} - \gamma_{w\alpha}) = (2/L)\gamma_{\alpha\beta}\cos\theta. \tag{8}$$

In the last step we have used Young's equation $\gamma_{w\beta} = \gamma_{w\alpha} + \gamma_{\alpha\beta}\cos\theta$ for the contact angle θ; $\gamma_{\alpha\beta}$ is the tension of the α–β interface at bulk α–β (liquid–gas) coexistence. Note that (8) is equivalent to Laplace's result for the pressure difference across the cylindrical meniscus that would develop between liquid and gas in a vertical slit; the mean radius of curvature is $L/\cos\theta$. A more convenient form of the result is obtained by expanding $p(\mu)$ about $p_\alpha^+(\mu)$ about p_{sat}. Condensation occurs when

$$\Delta\mu \equiv \mu_{sat} - \mu = 2\gamma_{\alpha\beta}\cos\theta/L(\rho_\alpha - \rho_\beta) \tag{9}$$

where ρ_α and ρ_β are the densities of the two coexisting bulk phases. When the gas is close to ideal $\Delta\mu \sim k_B T \ln(p_{sat}/p)$ and (9) reduces to the so-called Kelvin equation for the condensation pressure [3]. If the walls favour α (liquid), so that $\gamma_{w\alpha} < \gamma_{w\beta}$ and $\cos\theta > 0$, condensation occurs for $\mu < \mu_{sat}$ and the adsorption Γ jumps from a small value characteristic of gas adsorption by an amount [28] $\Delta\Gamma \sim (\rho_\alpha - \rho_\beta)L$, while the solvation force falls by an amount $\Delta f \sim -2\gamma_{\alpha\beta}\cos\theta/L$ consistent with (5). The physical picture of the transition is one in which the metastable α-phase is stabilized by surface tension; the fact that there are bulk and surface contributions to the grand potential gives $\Omega_\alpha < \Omega_\beta$ for non-zero $\Delta\mu$. If the walls favour gas, so that $\cos\theta < 0$, equation (9) predicts capillary evaporation of the liquid for some $\mu > \mu_{sat}$. This phenomenon is

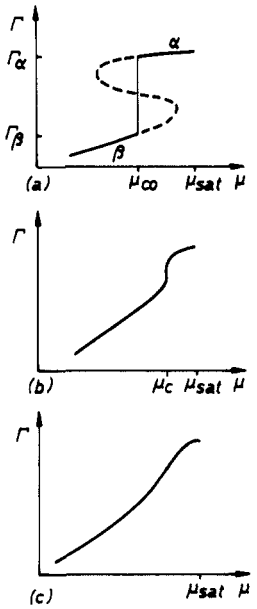

Figure 2. Schematic adsorption isotherms for a slit of fixed width L. (*a*) $T < T_{c,L}$. $\Gamma(\mu)$ exhibits a loop (broken curve) and the location of the equilibrium transition μ_{co} is given by an equal-area construction. (*b*) $T = T_{c,L}$. Γ has infinite slope at μ_c. (*c*) $T > T_{c,L}$.

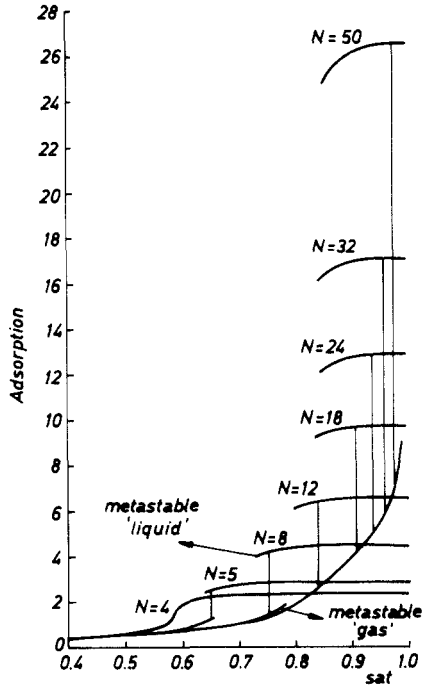

Figure 3. Adsorption isotherms for a lattice gas model with $T/T_{c,\infty} = 0.9$ and various numbers of layers N. The vertical portions represent the jump $\Delta\Gamma$ associated with capillary condensation. Note the existence of metastable 'gas' and 'liquid' branches. *sat* ($\approx p/p_{sat}$) measures the degree of undersaturation of the bulk gas—see [26].

relevant for mercury porisometry studies of porous solids [3]. Equation (9) should be the *exact* asymptotic ($L \to \infty$) law for the shift of *any* bulk first-order transition, provided the interfacial tensions and contact angle are identified properly. For cylindrical geometry L is replaced by R_c [12]. Sometimes it is more appropriate to focus on the shift of the bulk transition arising from confinement at fixed pressure rather than at fixed temperature. It is straightforward [28] to show that the resulting shift in the transition temperature is

$$\Delta T \equiv T - T_b = 2T_b(\gamma_{w\beta} - \gamma_{w\alpha})/Ll\rho_b$$

where l is the latent heat per mole and T_b is the temperature of the bulk transition. ρ_b is the density of the bulk phase with the lower interfacial tension. The result is equivalent to the standard formula for the shift in transition temperature arising from the curvature of the interface between the two coexisting phases. It has been invoked successfully, with L replaced by some mean pore radius, to explain the reduction of the freezing temperature measured for various liquids confined in VYCOR glass and in other porous solids [28, 33]. In this case $\gamma_{wl} < \gamma_{ws}$ where s refers to the crystalline phase. The same equation has been used [34–36] to interpret the shift of the isotropic–nematic transition in liquid crystal films. It can be generalized [28] to a phase-separating binary mixture.

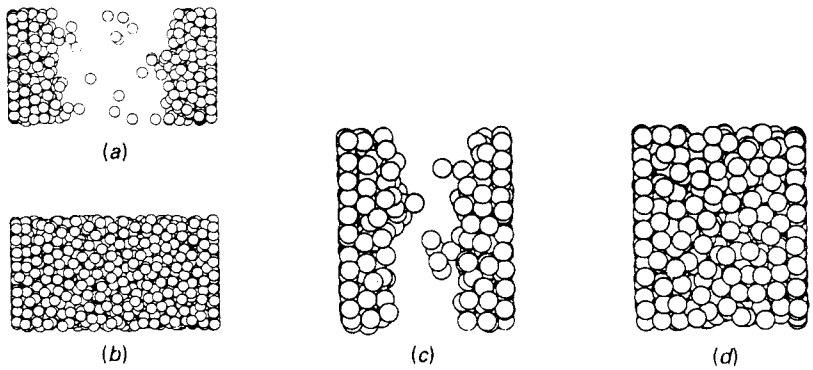

Figure 4. Snapshots of atomic configurations generated in GCMC simulations [23] of a Lennard-Jones fluid in a slit at $T = 0.71T_{c,\infty}$. (*a*) 'gas' at $p/p_{sat} = 0.90$, $L^* \equiv L/\sigma_{LJ} = 20$. (*b*) 'liquid' at $p/p_{sat} = 0.95$, $L^* = 20$. (*c*) 'gas' at $p/p_{sat} = 0.516$, $L^* = 10$. (*d*) 'liquid' at $p/p_{sat} = 0.516$, $L^* = 10$.

Then the shift in concentration, at fixed temperature and pressure, is proportional to $\gamma_{w\beta} - \gamma_{w\alpha}$ where α and β now refer to phases rich in species 2 and 1, respectively. How the phase separation curve is influenced by confinement depends on which of the two phases is preferred by the walls, i.e. on the wetting behaviour.

To what extent do these limiting laws remain valid for smaller pores? The regime of validity can be ascertained by comparing the results of microscopic theories, or computer simulations, with those of the limiting formulae, calculating the thermodynamic quantities $\gamma_{w\alpha}$ and $\gamma_{w\beta}$ etc from the same theory. This is of some practical importance for gas adsorption. The Kelvin equation is often used [3] to infer a pore radius from low temperature isotherms, where the rapid increase in Γ is identified with capillary condensation, even for pores with $R_c \sim$ few molecular diameters.

4.2. Results of microscopic treatments

Theory and simulation have concentrated on the liquid–gas transition for pure fluids and for binary Lennard-Jones mixtures [37, 38] in model pores.

Figure 3 shows the results of calculations of the adsorption Γ for the lattice gas model described by (1), with a *hcp* lattice. These particular results [26] are based on the mean-field approximation, but Monte Carlo results [21] for the same model exhibit similar features. The substrates are modelled by the 9–3 potential with ε_w chosen to represent argon adsorbed on solid xenon. As the number of layers N in the slit increases, capillary condensation occurs at increasing values of p/p_{sat} and the jump $\Delta\Gamma$ is roughly proportional to N for the larger systems. For $N \geqslant 12$ the adsorption on the gas branch is independent of N. The Kelvin equation overestimates the condensation pressure even for the largest slit, $N = 50$, where it is in error by about 40%. This type of discrepancy, although less pronounced at lower temperatures, is found for both lattice and continuum models in theory [11–13] and in simulation [21, 22, 25], when liquid wets the walls completely, i.e. $\theta = 0$. Under these circumstances thick, liquid-like films are adsorbed on the walls when the undersaturation is small. Figure 4 shows 'snapshots' of configurations from GCMC simulations [23] of capillary condensation for a Lennard-Jones model of (spherical) nitrogen between two graphite substrates modelled by the 9–3 potential. For

$L^* = 20$ the first three or four layers are essentially the same in both phases. Similarly for $L^* = 10$ the first two layers have the same structure in both phases. At a single wall ($L = \infty$) the thickness t of the adsorbed wetting film increases as $(\mu_{sat} - \mu)^{-1/3}$ for walls exerting van der Waals forces. The presence of such films in the slit leads to a modified Kelvin equation valid for large L:

$$\Delta\mu = 2\gamma_{\alpha\beta}/(L - 3t)(\rho_\alpha - \rho_\beta).$$

Here t depends on $\Delta\mu$ and, hence, L. That L should be replaced by $L - 3t$ rather than $L - 2t$, as would be suggested by a naive balancing of bulk and surface energies, was recognized first by Derjaguin [39] in 1940 and attests to the importance of long-ranged van der Waals forces in wetting phenomena. Only for exponential or finite-ranged forces is $L - 2t$ appropriate [39, 40].

The modified Kelvin equation does provide a somewhat more accurate estimation of the condensation pressure for large slits [21]. In a partial wetting situation, $\theta > 0$, where thick films are not present, the Kelvin equation remains accurate down to surprisingly small pore sizes. Mean-field calculations [26] for lattice models and density functional results for continuum fluids [20] indicate that the asymptotic formula remains very reliable for L or $R_c \geqslant 6$ molecular diameters or lattice spacings. It is still not clear why a formula based on macroscopic arguments should remain valid at microscopic dimensions; the density profiles of the confined liquid exhibit pronounced structure over the total pore volume [20].

Of course the Kelvin equation cannot describe other aspects of the phase equilibria. Reducing the slit width L leads to capillary criticality (vanishing $\Delta\Gamma$), provided the temperature is above the two-dimensional critical temperature $T_{c,1}$. The $N = 4$ isotherm in figure 3 is slightly supercritical. The loss of phase coexistence at small L and R_c has been observed in many density functional calculations [11–13] and computer simulations [22, 25] of continuum fluids. The variable $1/L$, or $1/R_c$, plays a similar role to the temperature in inducing criticality of the confined fluid so that one finds a line of critical points [11, 26] $(\mu_{c,L}, T_{c,L})$, with $T_{c,L} < T_{c,\infty}$, extending into the bulk gas phase when $\cos\theta > 0$ or into the bulk liquid phase when $\cos\theta < 0$.

For very narrow *slits* two-dimensional-like phase equilibria are found. In the lattice model, coexistence of strictly two-dimensional 'liquid' and 'gas' phases occurs for a single layer, $N = 1$, provided $T < T_{c,1}$, for $\mu = -V_1 + \mu_c^{2D}$ with $\mu_c^{2D} = -2\varepsilon$ the chemical potential at saturation for a square Ising lattice. The non-local density functional approach can describe two-dimensional phase coexistence for continuum models in the limit where $L \to 0$ [20, 41]. The same theory yields an excellent description of the density profile of liquids confined in narrow cylindrical pores [42]—see figure 5. It reproduces all the structure associated with packing effects that is found in simulation [43] of the same model. Moreover, it gives an adequate description of the one-dimensional fluid behaviour expected when the radius $R_c \to 0$ [25].

Note that the simulation results [22, 25, 43] provide evidence for sharp condensation transitions, even in narrow cylinders. At first sight this is surprising. Since the geometry is equivalent to that of an infinite strip, true phase transitions cannot occur for $T > 0$. Any first-order transition must be rounded by finite-size effects [44]. A crude estimate [14] shows that the rounding in $\Delta\mu$ is on the scale $\exp(-(R_c/\sigma_{LJ})^2)$, where σ_{LJ} is a molecular diameter. Thus even for $R_c = 3\sigma_{LJ}$ the transition appears to be very sharp. Another consequence of the finite cross-sectional area of an interface in a cylinder should be the occurrence, along the axis, of a series of alternating domains [44] of the two 'quasi'-coexisting phases rather than a single domain of each. A series of ten different

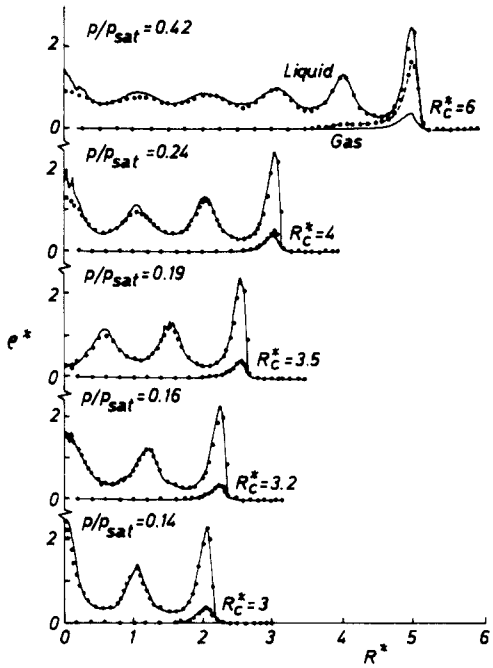

Figure 5. Radial density profiles $\rho^* = \rho(R)\sigma_{LJ}^3$ for coexisting phases of a Lennard-Jones fluid in cylindrical pores of different radii $R_c^* = R_c/\sigma_{LJ}$. The potential parameters are chosen to model argon at a solid CO_2 substrate. In each case the oscillatory profiles correspond to 'liquid'. Full curves denote simulation results [43] and the dotted curves denote results of density functional calculations. $T/T_{c,\infty} = 0.61$. Note the variation of the central density $\rho(0)$ as R_c is decreased. The relative pressure at which condensation occurs is given for each radius—see [42].

'gas' and 'liquid' domains has been observed in molecular dynamics simulations with very long pore lengths [24, 38].

Returning to slits, where true phase transitions do occur, a scaling argument [45] predicts that in the limit $L \to \infty$ the critical point shift $\Delta T_c(L) \equiv (T_{c,\infty} - T_{c,L})/T_{c,\infty} \sim L^{-1/\nu}$, where $\nu \approx 0.63$ is the bulk (three-dimensional) correlation length exponent. The growth of droplets is determined by bulk critical fluctuations until the droplet size is comparable with the smallest dimension of the system, i.e. at $T_{c,L}$, $\xi_b \sim (T_{c,\infty} - T)^{-\nu} \sim L$. The scaling prediction has been confirmed in Monte Carlo simulations of Ising lattices with free boundaries [46]. For small values of L, $\Delta T_c(L)$ varies roughly as $1/L$ [26]. Capillary criticality is of special interest since it corresponds to the *two-dimensional* Ising universality class. At $T = T_{c,L}$ the correlation length $\xi_\parallel$ that measures the range of fluctuations in density can diverge parallel to the walls of the slit but not normal to them. Thus, on a critical isotherm, such as that sketched in figure 2(*b*), the adsorption should take the form $|\Gamma - \Gamma_c| \sim |\mu - \mu_c|^{1/\delta}$ with critical exponent $\delta = 15$. This gives rise to a much faster divergence of $(\partial\Gamma/\partial\mu)$ than the mean-field result which has $\delta = 3$. Note that in three dimensions $\delta \approx 4.81$. Moreover, the jump in adsorption should vanish as $\Delta\Gamma \sim (T_{c,L} - T)^\beta$ with order parameter exponent $\beta = \frac{1}{8}$, rather than with the mean-field value $\beta = \frac{1}{2}$ or the three-dimensional value $\beta \simeq 0.32$. To the best of

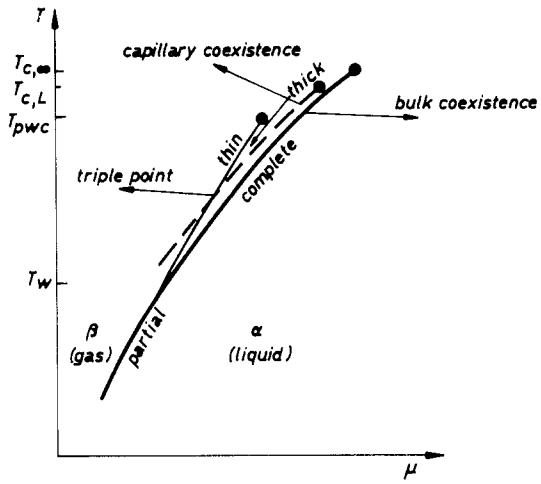

Figure 6. A schematic phase diagram for a fluid exhibiting a first-order wetting transition at T_w. The prewetting line, where thin and thick films coexist, meets the bulk gas–liquid coexistence curve $\mu_{sat}(T)$ tangentially at T_w. In the confined system the bulk coexistence curve is shifted to $\mu < \mu_{sat}$ (broken curve) and a triple point occurs where this line crosses the prewetting line. Note that the prewetting critical temperature T_{pwc} is distinct from the capillary critical temperature $T_{c,L}$.

our knowledge such predictions have not been tested in simulations although the two-dimensional character of the somewhat analogous *surface* (prewetting) critical point has been confirmed [47] in extensive Monte Carlo calculations for a lattice gas model.

5. Surface phase transitions in pores: prewetting and layering

Capillary condensation is not the only transition that can occur in pores. Confining a fluid precludes the roughening and wetting transitions [18, 19] that take place at the interface between two semi-infinite bulk phases. The wetting transition, for example, is associated with the growth of a macroscopic film, $t \rightarrow \infty$, of α-phase at the interface between a substrate (or spectator phase) and the bulk β-phase as T is increased towards T_w, the wetting transition temperature, along the bulk coexistence curve—see figure 6. For $T \geqslant T_w$ complete wetting occurs and $\gamma_{w\beta} = \gamma_{w\alpha} + \gamma_{\alpha\beta}$. If the fluid is confined within a slit or cylinder, films of macroscopic thickness cannot develop. However, those surface transitions which occur out of bulk coexistence, $\mu < \mu_{sat}$, for a semi-infinite system ($L = \infty$) are not precluded since these do not require thickness $t \rightarrow \infty$. Examples of such transitions are prewetting and layering [18]. The former is associated with weak substrates where $\varepsilon_w \geqslant \varepsilon$, whereas the latter occurs when $\varepsilon_w \gg \varepsilon$.

If the wetting transition, for $L = \infty$, is first order so that t, or Γ, jumps discontinuously from a microscopic to a macroscopic value at $T = T_w$, a line of first-order prewetting or thin–thick transitions [48, 49] extends away from $\mu_{sat}(T)$ as shown in figure 6. Prewetting is characterized by a single discontinuous jump $\Delta\Gamma$ in the adsorption for μ slightly less than μ_{sat} and $T_w < T < T_{pwc}$. For $T \geqslant T_w$, $\Delta\Gamma$ is very large, corresponding to several adsorbed layers, but at the prewetting critical point T_{pwc} $\Delta\Gamma$ vanishes, since there is no longer any distinction between thin and thick adsorbed films. When L (or R_c) is large,

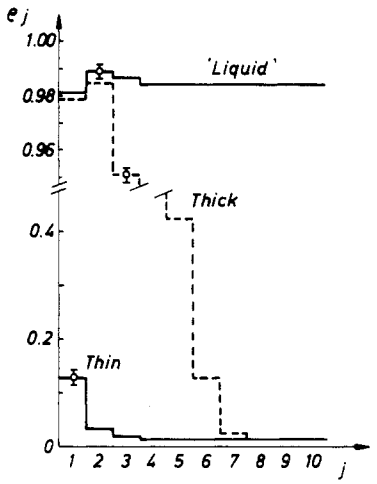

Figure 7. The density (occupancy) profiles ρ_j for the triple-point state of a lattice gas model. These Monte Carlo results [21] are for a slit with $N = 61$ layers. $T/T_{c,\infty} = 0.588$. Only the first ten layers near one wall are shown. Representative errors bars are indicated.

but finite, prewetting will still occur, at much the same undersaturation $\Delta\mu_{pw}$ as before, but will now be in competition with capillary condensation. Confinement shifts the bulk coexistence curve by an amount $\Delta\mu \sim 1/L$ for large L and lowers the bulk critical temperature to $T_{c,L}$ (see figure 6). Thus prewetting between stable phases will not be observed [50] unless $\Delta\mu < \Delta\mu_{pw}$. This condition requires large pores since the undersaturation $\Delta\mu_{pw}$, even at T_{pwc}, is only a few per cent [21, 26]. The prewetting and condensation lines intersect in a triple point; the three coexisting fluid phases are thin and thick adsorbed films plus a dense 'liquid' that fills the pore. An example [21] of such a state is shown in figure 7 for a lattice gas model. Similar results are obtained from density functional calculations for continuum fluids in slits and cylinders [12, 50]. By varying the pore size a line of triple points, as well as lines of capillary and prewetting critical points, emerge and the resulting phase diagram, plotted in terms of $(\mu, T, 1/L)$, is predicted to be rather rich [26, 50]. Thermodynamic arguments given in III explain why three fluid phases can coexist out of bulk coexistence. The surface tension term $2\gamma\,\mathrm{d}A$ in (2) accounts for the thin–thick coexistence while the solvation force term $-Af\,\mathrm{d}L$ accounts for capillary condensation.

While prewetting has not been observed in any real experiment, discrete layering transitions, whereby the adsorption jumps discontinuously from Γ_n to Γ_{n+1} by an amount corresponding to a single new layer, have been found in many experiments for rare gases or small molecules adsorbed on graphite. For example, as many as eight first-order layering transitions have been measured for argon on graphite along isotherms just below the bulk triple point [51, 52]. As $\mu \to \mu_{sat}$ it becomes increasingly difficult to discern the transitions because (i) they occur at closely spaced values μ_n and (ii) the possibility of capillary condensation occurring on powder substrates, such as exfoliated graphite, arises. Indeed the higher-order layering transitions compete with condensation in much the same way as prewetting does. Calculations [26] for lattice models using larger values of ε_w than those which yield prewetting show that while the location μ_n of the layering transitions is not affected strongly by confinement, only six stable transitions survive before condensation occurs in slits with 100 layers. Triple points can occur where capillary condensed 'liquid' coexists with films of n and $n + 1$ adsorbed layers. Layering transitions competing with condensation have also been investigated for continuum fluids confined in cylinders [53, 66]. Although the finite-size rounding of layering and

prewetting is of a somewhat different character [14] from that of condensation, both should persist as very sharp transitions even in narrow cylindrical pores. Finally, it should be emphasized that while the critical points of layering or prewetting transitions are believed to lie in the same universality class as that of the capillary condensation critical point discussed earlier, these surface critical points are quite distinct from the shifted bulk critical point.

6. Concluding remarks and relevance for experiment

As emphasized in the introduction, this article has concentrated on the equilibrium properties of simple, one-component fluids confined in highly idealized pores. Theory and simulation have made striking advances during the last six or seven years leading to predictions of novel phase diagrams† and of complex microscopic structure for confined fluids. Having established some fundamental understanding of what type of *phenomena* might be expected to occur in pores, the time is probably right for detailed simulations using more realistic model potentials. These would provide more information about capillary freezing [8, 9] and dynamical properties [5, 6]. Extending theory and simulation to describe binary mixtures in pores is relatively straightforward but only a few studies have been reported [37, 38, 54]. The new ingredient is the existence of preferential adsorption of one species with respect to another arising from differences in substrate–fluid attraction and from the difference in size of the fluid molecules. The composition of a fluid in a narrow pore can be significantly different from that in bulk and this may have implications for separation processes.

Direct comparison of theory and experiment is not straightforward. Ideal pores with the relevant dimensions are not easy to come by. Studies based on liquids between crossed mica cylinders provide some of the more relevant results. Fisher and Israelachvili [63] tested the validity of the Kelvin equation by allowing cyclohexane to condense between the two cylinders which were then separated until the liquid bridge became unstable. The maximum value of the separation determines the mean radius of curvature of the bridging neck for a given p/p_{sat}. For this system, which has a non-zero contact angle $\theta \sim 6°$, they conclude that the Kelvin equation (employing the planar liquid–gas tension) remains accurate down to separations ~80 Å, or 16 molecular diameters. This result is in keeping with the theoretical estimates described earlier. Later Christenson and co-workers investigated the spontaneous phase separation of a binary liquid mixture. For a sparingly soluble liquid solute the analogue of the Kelvin equation for the activity a at which separation occurs is $\ln a = -2\gamma_{\alpha\beta} \cos\theta / k_B T L \rho_\alpha$ where $\gamma_{\alpha\beta}$ is the tension between the pure α-phase and the dilute solution β, θ is the corresponding contact angle with the substrate and ρ_α is the number density of pure α [28]. Their most recent study [64] considers non-polar liquids containing water held between the mica cylinders. The two surfaces are allowed to approach each other and the separation at which spontaneous phase separation occurs is measured as a function of the activity of the dissolved species (water). This process is signalled by an inward jump of the surfaces into contact. The

† In this article we considered fluids confined between identical parallel walls. When the two walls exert different (competitive) surface fields the phase equilibria of the confined fluid can be very different [60] from that for equal fields. In particular, if the surface fields and temperature are such that the fluid would wet one wall but dry the other, there can be no phase coexistence for finite wall separation L; the critical point shift is of a very different character from that described in section 4, being driven by wetting behaviour [60].

distance at which the jump occurs is independent of the spring constant of the surface force apparatus [64]. In these measurements, at high water activity, the solvation force is very weak at large separations but the spontaneous separation results in a very large attraction. At water activities below 0.75 [65] an oscillatory solvation force is present until spontaneous phase separation occurs, again leading to a sudden attraction. By plotting the separation distance against the activity, the analogue of the Kelvin equation can be tested. There is qualitative agreement with theory for separations between about 40 and 130 Å for octamethylcyclotetrasiloxane (OMCTS) and natural potassium mica, corresponding to activities in the range 0.8 to 0.95. For larger activities the condensing water bridges are large and their formation depends on kinetic and diffusion effects. Christenson *et al* [64] argue that their data are the most direct experimental observations of phase transitions in very thin films and they interpret their results as direct evidence for a first-order phase transition of the confined liquid. They are careful to point out that the force that is measured when the surfaces jump together is not f_β appropriate to the phase-separated (water) phase; the quantity that would be obtained from a theory of the first-order transition is the jump in force $\Delta f = f_\alpha - f_\beta$. The measured attractive force results from the formation of a liquid–liquid interface of negative curvature which pulls the surfaces together. Nevertheless, the technique does appear to provide a powerful means of locating shifted bulk transitions. Some hysteresis with respect to increasing/decreasing the separation of the cylinders is observed, reflecting possible metastabilities of the transition.

Do the results obtained for single pores have any relevance for gas adsorption on real porous solids containing a complex network of interconnected pores of various shapes and sizes? This is really a separate topic. For example, capillary condensation certainly occurs in materials such as VYCOR and gives rise to hysteresis of the adsorption isotherms. Whether the measured hysteresis is due primarily to the existence of metastable states in a single pore (cf figures 2 and 3) or to pore blocking—i.e. evaporation of the capillary condensate, which should occur spontaneously during desorption, is obstructed by 'liquid' condensed in constrictions or 'necks'—is still a matter for some debate. Recent calculations [55] for a model of Xe on VYCOR and comparison with experiment [56] support the view that pore blocking, arising from network effects, determines the shape of the hysteresis loops and is responsible for the form of desorption scanning curves, obtained by decreasing the pressure before saturation is reached. Much more theoretical effort is required in this area. While it has been shown, via a lattice gas calculation, that hysteresis in a single pore of *finite* length reflects the development of a meniscus [57], it is not easy to incorporate network effects at the microscopic level.

The dependence of adsorption on temperature has been studied systematically for only a few cases. Isotherms for Xe on VYCOR [56], and for closely related systems, show hysteresis loops shrinking with increasing temperature and eventually disappearing at some temperature below $T_{c,\infty}$. This is illustrated in figure 8. Ball and Evans [55] and Everett [58] have interpreted such behaviour as evidence for a capillary critical point whose location depends on the average pore size. Figure 9 shows the results of calculations [55] for a network model which assumes a Gaussian pore size distribution, with average cylinder radius $R_A = 29.4$ Å and a standard deviation of $0.2\,R_A$. It is assumed there is no metastability for a single pore so that all the hysteresis is associated with network efects and these are treated in the same spirit as in the work of Mason [59]. The disappearance of the loops in these calculations reflects the decrease in the jump in $\Delta\Gamma$ at capillary condensation as criticality is approached—see section 4. Although there is rough agreement with the experimental results of figure 8 (the loop disappears at about

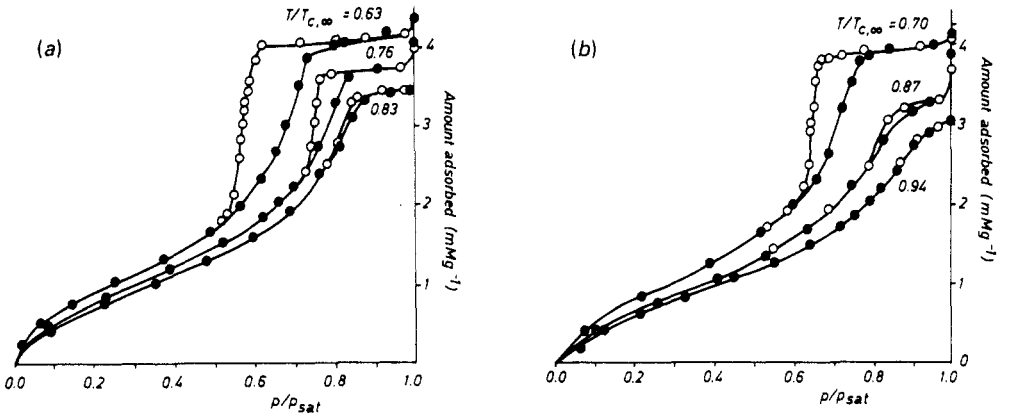

Figure 8. Adsorption isotherms of Xe on VYCOR [56]. Full circles denote adsorption; open circles denote desorption. $T_{c,\infty} = 289.7$ K is the bulk critical temperature of Xe. At the highest temperature $T/T_{c,\infty} = 0.94$ no hysteresis is observed.

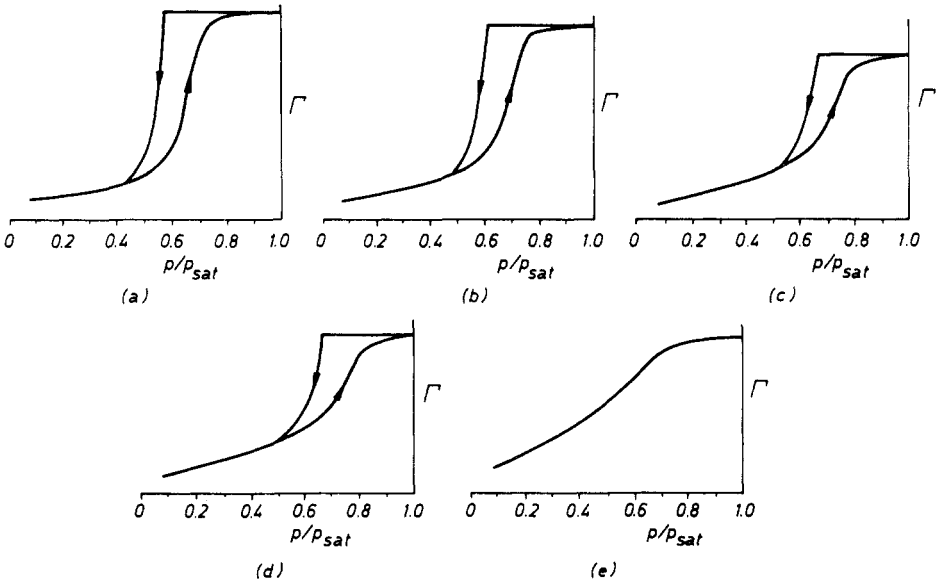

Figure 9. Adsorption isotherms calculated for the network model described in [55]. Γ is given in arbitrary units. (*a*) $T = 0.63T_{c,\infty}$; (*b*) $T = 0.70T_{c,\infty}$; (*c*) $T = 0.83T_{c,\infty}$; (*d*) $T = 0.87T_{c,\infty}$; (*e*) $T = 0.94T_{c,\infty}$. Note that the sharp kink on desorption is an artifact of the model; this would be rounded in a more realistic treatment.

the same value of $T/T_{c,\infty}$) there are also important discrepancies [55]. These might be attributed to the crudeness of the network model. Ideally the theoretician would like to have adsorption data for a material with uniform, preferably unconnected, pores of known radius, rather than for the poorly characterized VYCOR or silica gels. This is a tall order! It remains to be seen whether suitable materials can be produced using

techniques such as electron beam boring or whether certain zeolite crystals would be good candidates.

Acknowledgments

Part of this article was prepared while the author was visiting the Katholieke Universiteit Leuven. The hospitality of J O Indekeu and his colleagues in physics is gratefully acknowledged. The author also wishes to thank his co-workers P C Ball, D Nicolaides, A O Parry, U Marini Bettolo Marconi and P Tarazona for simulating collaborations, his colleague D H Everett for introducing him to the subject and H K Christenson and J N Israelachvili for informative discussions. This research was supported by the SERC.

References

[1] Rowlinson J S and Widom B 1982 *Molecular Theory of Capillarity* (Oxford: Oxford University Press)
[2] Nicholson D and Parsonage N G 1982 *Computer Simulation and the Statistical Mechanics of Adsorption* (New York: Academic)
[3] Gregg S J and Sing K S W 1982 *Adsorption, Surface Area and Porosity* (New York: Academic)
[4] Israelachvili J N 1987 *Acc. Chem. Res.* **20** 415
[5] Bitsanis I, Vanderlick T K and Davis H T 1988 *J. Chem. Phys.* **89** 3152
[6] Schoen M, Cushman J H, Diestler D J and Rhykerd C L 1988 *J. Chem. Phys.* **88** 1394
[7] Woods G B, Panagiotopoulos A Z and Rowlinson J S 1988 *Mol. Phys.* **63** 49
[8] Schoen M, Diestler D J and Cushman J H 1987 *J. Chem. Phys.* **87** 5464
[9] Rhykerd C L, Schoen M, Diestler D J and Cushman J H 1987 *Nature* **330** 461
[10] Tan Z and Gubbins K E 1990 *J. Chem. Phys.* at press
[11] Evans R, Marini Bettolo Marconi U and Tarazona P 1986 *J. Chem. Phys.* **84** 2376
[12] Evans R, Marini Bettolo Marconi U and Tarazona P 1986 *J. Chem. Soc. Faraday Trans. II* **82** 1763
[13] Peterson B K, Walton J P R B and Gubbins K E 1986 *J. Chem. Soc. Faraday Trans. II* **82** 1789
[14] Evans R 1990 *Liquids at Interfaces (Les Houches Session XLVIII)* ed J Charvolin, J Joanny and J Zinn-Justin (Amsterdam: Elsevier)
[15] Hill T L 1947 *J. Chem. Phys.* **15** 767
[16] Nicholson D 1975 *J. Chem. Soc. Faraday Trans. I* **71** 239
[17] Goldstein R E and Parola A 1989 *Acc. Chem. Res.* **22** 77
[18] Sullivan D E and Telo da Gama M M 1986 *Fluid Interfacial Phenomena* ed C A Croxton (New York: Wiley) p 45
[19] Dietrich S 1988 *Phase Transitions and Critical Phenomena* vol 12, ed C Domb and J L Lebowitz (New York: Academic) p 1
[20] Tarazona P, Marini Bettolo Marconi U and Evans R 1987 *Mol. Phys.* **60** 573
[21] Nicolaides D and Evans R 1989 *Phys. Rev.* B **39** 9336
[22] Peterson B K and Gubbins K E 1987 *Mol. Phys.* **62** 215
[23] Walton J P R B and Quirke N 1989 *Mol. Simul.* **2** 361
[24] Heffelfinger G S, van Swol F and Gubbins K E 1988 *J. Chem. Phys.* **89** 5202
[25] Peterson B K, Gubbins K E, Heffelfinger G S, Marini Bettolo Marconi U and van Swol F 1988 *J. Chem. Phys.* **88** 6487
[26] Bruno E, Marini Bettolo Marconi U and Evans R 1987 *Physica* A **141** 187
[27] Tarazona P 1985 *Phys. Rev.* A **31** 2672
[28] Evans R and Marini Bettolo Marconi U 1987 *J. Chem. Phys.* **86** 7138
[29] Derjaguin B V, Churaev N V and Müller V M 1987 *Surface Forces* (New York: Consultants Bureau)
[30] Horn R and Israelachvili J N 1980 *Chem. Phys. Lett.* **71** 192
[31] Henderson J R 1986 *Mol. Phys.* **59** 89
[32] Zsigmondy R 1911 *Z. Anorg. Allg. Chem.* **71** 356
[33] Warnock J, Awschalom D and Shafer M W 1986 *Phys. Rev. Lett.* **57** 1753
[34] Sluckin T J and Poniewerski A 1986 *Interfacial Fluid Phenomena* ed C A Croxton (New York: Wiley) p 215

[35] Allen M P 1989 *Mol. Simul.* **4** 61
[36] Telo da Gama M M, Tarazona P, Allen M P and Evans R 1990 *Mol. Phys.* at press
[37] Heffelfinger G S, Tan Z, Gubbins K E, Marini Bettolo Marconi U and van Swol F 1989 *Mol. Simul.* **2** 393
[38] Heffelfinger G S, Tan Z, Gubbins K E, Marini Bettolo Marconi U and van Swol F 1988 *Int. J. Thermophys.* **9** 1051
[39] Derjaguin B V 1940 *Acta Phys. Chem.* **12** 181
[40] Evans R and Marini Bettolo Marconi U 1985 *Chem. Phys. Lett.* **114** 415
[41] Adams P, Henderson J R and Walton J P R B 1989 *J. Chem. Phys.* **91** 7173
[42] Ball P C and Evans R 1988 *Mol. Phys.* **63** 159
[43] Panagiotopoulos A Z 1987 *Mol. Phys.* **62** 701
[44] Privman V and Fisher M E 1983 *J. Stat. Phys.* **33** 385
[45] Fisher M E and Nakanishi H J 1981 *J. Chem. Phys.* **75** 5857
[46] Binder K 1974 *Thin Solid Films* **20** 367
[47] Nicolaides D and Evans R 1989 *Phys. Rev. Lett.* **63** 778
[48] Cahn J W 1977 *J. Chem. Phys.* **66** 3667
[49] Ebner C and Saam W F 1977 *Phys. Rev. Lett.* **38** 1486
[50] Evans R and Marini Bettolo Marconi U 1985 *Phys. Rev.* A **32** 3817
[51] Youn H S and Hess G B 1990 *Phys. Rev. Lett.* **64** 919
[52] Ser S, Larher Y and Gilquin B 1989 *Mol. Phys.* **67** 1077
[53] Ball P C and Evans R 1988 *J. Chem. Phys.* **89** 4412
[54] Tan Z, van Swol F and Gubbins K E 1987 *Mol. Phys.* **62** 1213
[55] Ball P C and Evans R 1989 *Langmuir* **5** 714
[56] Nuttall S 1974 *PhD Thesis* University of Bristol
[57] Marini Bettolo Marconi U and van Swol F 1989 *Phys. Rev.* A **39** 4109
[58] Everett D H 1988 *Proc. 5th Hungarian Colloid Conf.*
[59] Mason G 1983 *Proc. R. Soc.* A **390** 47
[60] Parry A O and Evans R 1990 *Phys. Rev. Lett.* **64** 439
[61] Zhou Y and Stell G 1990 *J. Chem. Phys.* **92** 5544
[62] Kjellander R and Sarman S 1990 *Mol. Phys.* **70** 215
[63] Fisher L R and Israelachvili J N 1981 *J. Colloid Interface Sci.* **80** 528
[64] Christensen H K, Fang J and Israelachvili J N 1989 *Phys. Rev.* B **39** 11750
[65] Christensen H K and Blom C E 1987 *J. Chem. Phys.* **86** 419
[66] Peterson BK, Heffelfinger GS, Gubbins KE and van Swol F 1990 *J. Chem. Phys.* **93** 679